

Giant dielectric relaxation in $\text{SrTiO}_3\text{-SrMg}_{1/3}\text{Nb}_{2/3}\text{O}_3$ and $\text{SrTiO}_3\text{-SrSc}_{1/2}\text{Ta}_{1/2}\text{O}_3$ solid solutions

© V.V. Lemanov*, A.V. Sotnikov*,**, E.P. Smirnova*, M. Wehnacht**

* A.F. Ioffe Physical-Technical Institute,
194021 St.Petersburg, Russia

** Leibniz Institute of Solid State and Materials Research Dresden,
D-01069 Dresden, Germany

(Received 11 April 2002)

Ceramic samples of $(1-x)\text{SrTiO}_3\text{-}x\text{SrMg}_{1/3}\text{Nb}_{2/3}\text{O}_3$ and $(1-x)\text{SrTiO}_3\text{-}x\text{SrSc}_{1/2}\text{Ta}_{1/2}\text{O}_3$ were prepared and their dielectric properties were studied at $x = 0.005\text{--}0.15$ and $0.01\text{--}0.1$, respectively, at frequencies $10\text{ Hz--}1\text{ MHz}$ and at temperatures $4.2\text{--}350\text{ K}$. A giant dielectric relaxation was observed in the temperature range $150\text{--}300\text{ K}$, and not so strong but well-developed relaxation was found in the temperature range $20\text{--}90\text{ K}$. The activation energy U and the relaxation time τ_0 were determined to be $0.21\text{--}0.3\text{ eV}$ and $10^{-11}\text{--}10^{-12}\text{ s}$ for the high-temperature relaxation and $0.01\text{--}0.02\text{ eV}$ and $10^{-8}\text{--}10^{-10}\text{ s}$ for the low-temperature relaxation. The additional local charge compensation of the heterovalent impurities Mg^{2+} and Nb^{5+} (or Sc^{3+} and Ta^{5+}) by free charge carriers or the host ion vacancies is suggested as underlying physical mechanism of the relaxation phenomena. On the base of this mechanism, the Maxwell-Wagner model and the model of reorienting dipole centers Mg^{2+} (or Sc^{3+}) associated with the oxygen vacancy are proposed to explain the high-temperature relaxation with some arguments in the favour of the latter model. The polaron-like model with the $\text{Nb}^{5+}\text{-Ti}^{3+}$ center is suggested as the origin of the low-temperature relaxation. The reasons of no ferroelectric phase transitions in the solid solutions under study are also discussed.

Strontium titanate, SrTiO_3 , is known to be an incipient ferroelectric and a quantum paraelectric [1]. The SrTiO_3 crystal has a polar soft mode but never exhibits a ferroelectric phase transition down to $T = 0$ due to quantum fluctuations. At low temperatures, the dielectric constant in SrTiO_3 attains very high values. According to [2], $\epsilon_a = 41\,900$ and $\epsilon_c = 9380$ (4 K , $1\text{--}100\text{ kHz}$). It should be noted that these remarkable values were obtained by extrapolation of the inverse susceptibility versus stress to zero stress, and later on nobody was able to reproduce this result directly. More or less typical experimental values of ϵ_a in direct measurements instead of $41\,900$ is around $20\,000$, and even this value is remarkable.

The SrTiO_3 crystal may be considered as a marginal system which is near the limit of its paraelectric phase stability. Small external perturbations such as elastic stress or impurities can destroy the stability and induce a ferroelectric phase transition. Various impurities substituted for the host ions in SrTiO_3 both in the A - and B -position have been studied [3,4]. It was shown that divalent impurities substituting for Sr^{2+} such as Ca [5], Ba [6], Pb [7] and Cd [8] induce a ferroelectric phase transition with the transition temperature T_c proportional to $(x-x_c)^{1/2}$ where the critical concentration x_c is about 0.002 and is almost the same for all these impurities with some specific features for the case of Ba . It appeared that isoivalent B -impurities (Zr , Sn , Ge) have much smaller effect on dielectric properties of SrTiO_3 . Simultaneous substitution of the host Sr^{2+} and Ti^{4+} ions by impurity ions give some specific effects. For example, in $\text{SrTiO}_3\text{-PbMg}_{1/3}\text{Nb}_{2/3}\text{O}_3$ (PMN) solid solution the transition to a ferroelectric phase (with relaxor properties) was observed only at $x > 0.2$

with a linear dependence of T_c on x which was associated with random fields due to disordered Mg^{2+} and Nb^{5+} distribution [9].

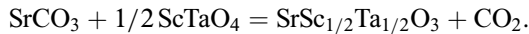
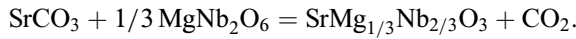
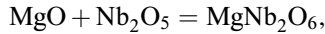
Quite different situation takes place for heterovalent impurities. In this case, instead of induced ferroelectric phase transitions, distinct dielectric relaxation is observed. (Maybe the only exclusion is $\text{SrTiO}_3\text{:Bi}^{3+}$; in [10] the authors claim that the Bi impurity induces a ferroelectric phase transition with $x_c = 0.0005$). There is a very long story of studying dielectric relaxation in SrTiO_3 with various heterovalent impurities: Bi [11–16], La [17–21], La and a wide range of other trivalent rare-earth ions [22], Fe [23,24].

In this paper, we studied some special case of heterovalent substitution when the host Ti^{4+} ion is substituted by two heterovalent ions whose average charge is equal to that of Ti^{4+} ion. As an example of such systems, the solid solutions of SrTiO_3 with $\text{SrMg}_{1/3}\text{Nb}_{2/3}\text{O}_3$ (SMN) and with $\text{SrSc}_{1/2}\text{Ta}_{1/2}\text{O}_3$ (SST) were chosen. The $\text{SrTiO}_3\text{-SMN}$ system, contrary to $\text{SrTiO}_3\text{-PMN}$, does not contain ferroelectrically active Pb^{2+} ions. A giant dielectric relaxation and no ferroelectric phase transition have been found in these solid solutions. Preliminary results of this study has been published elsewhere [25]. In the present paper, the giant relaxation in $(1-x)\text{SrTiO}_3\text{-}x\text{SMN}$ and $(1-x)\text{SrTiO}_3\text{-}x\text{SST}$ has been studied in detail.

1. Experimental procedure

Ceramic samples of SMN, SST, and $(1-x)\text{SrTiO}_3\text{-}x\text{SMN}$ and $(1-x)\text{SrTiO}_3\text{-}x\text{SST}$ solid solutions were prepared by a standard ceramic technology. Stoichiometric mixture of strontium carbonate and of Ti , Mg , Nb , Sc ,

and Ta oxides of a special purity were used to prepare the appropriate compounds and solid solutions. The pure compounds of SMN and SST were synthesized through a columbite (MgNb_2O_6) and a wolframite (ScTaO_4) route, respectively, according to the reactions



The columbite and wolframite were synthesized at 1000 and at 1200°C, respectively for 20 hours. After calcining the mixture at about 1200°C for several hours, the material was reground and pellets were formed by pressing 9 mm diameter disks at 200 MPa. The final sintering was proceeded at 1450°C for 1.5 h. X-ray diffraction study indicated that the samples had single-phase cubic perovskite structure up to the concentration $x = 0.15$ in the case of SMN and more than $x = 0.2$ in the case of SST.

The symmetry of the $\text{SrMg}_{1/2}\text{Nb}_{2/3}\text{O}_3$ crystal is known [26] to be rhombohedral with D_{3d}^3 space group with lattice parameters $a = 5.66$ and $c = 6.98$ Å. The parameter of reduced perovskite pseudocubic cell is $a = 4.01$ Å. With the SrTiO_3 parameter $a = 3.905$ Å, one obtains 2.7% difference between SrTiO_3 and SMN. At such a small difference in the lattice parameters one could expect the possibility to obtain the whole range of the $\text{SrTiO}_3\text{-SMN}$ solid solutions. However, the experiment shows that there is the solubility limit at the SMN concentration between 0.15 and 0.20. This low solubility may be attributed to the different crystal structure.

The lattice parameter of the $\text{SrTiO}_3\text{-SMN}$ solid solutions was measured, and it appeared that the lattice parameter follows a linear Vegard law between $a = 3.905$ (SrTiO_3) and 4.01 Å (SMN perovskite pseudocubic cell) with the slope $da/dx = 0.105$ Å.

The symmetry of the $\text{SrSc}_{1/2}\text{Ta}_{1/2}\text{O}_3$ crystal, as far as we can know, has not been determined earlier but the symmetry of closely related compound, $\text{SrSc}_{1/2}\text{Nb}_{1/2}\text{O}_3$ (SSN) is known [27] to be cubic with O_h^5 space group; the compound has ordered perovskite structure with the doubled unit cell parameter $a = 8.057$ Å.

According to our measurements the lattice parameter of SST is equal to $a = 8.054 \pm 0.003$ Å, i.e. very close to the SSN lattice parameter. This allows us to conclude that these compounds are isomorphic with the O_h^5 space group.

The x-ray measurement demonstrated that the lattice parameter in $(1-x)\text{SrTiO}_3\text{-}x\text{SST}$ solid solutions also follows a linear Vegard law between $a = 3.905$ (SrTiO_3) and 4.027 Å (SST perovskite reduced cell) with the slope $da/dx = 0.12$ Å. The lattice parameter difference between SrTiO_3 and SST is 3.1%. Though this difference is a little bit higher than that between SrTiO_3 and SMN, this solid

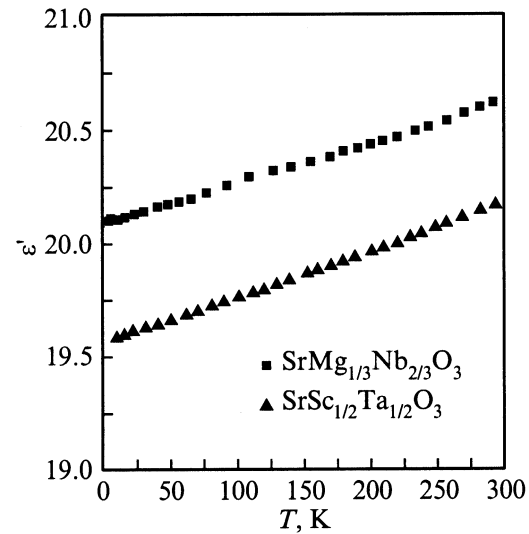


Figure 1. Temperature dependence of the dielectric constant ϵ' in $\text{SrMg}_{1/3}\text{Nb}_{2/3}\text{O}_3$ and $\text{SrSc}_{1/2}\text{Ta}_{1/2}\text{O}_3$.

solution exists in a much broader range of SST concentration due to the similar crystal structure.

All the samples had density between 92 and 97% with regard to the theoretical x-ray density. Pure SMN and SST samples had density of about 87%. The samples for dielectric measurements had a diameter of 8 mm and a thickness of 1–0.4 mm. For the measurements the samples were coated with silver burnt, gold evaporated and In–Ga alloy-electrodes. In all cases we obtained absolutely the same results (within small experimental errors) on the temperature and frequency dependences of the dielectric constant. The dielectric constant was measured using a Solartron SI 1260 Impedance/Gain-Phase Analyzer interfaced with a computer. The measurements were performed at frequencies between 10 Hz and 1 MHz, in a temperature range between 4.2 and 300 K by cooling at a constant rate of 1 K/min. The amplitude of a.c. electric field was 1 V/cm.

2. Experimental results and analysis

The temperature dependence of the real part ϵ' of the dielectric constant in SMN and SST ceramic samples is shown in Fig. 1. In both materials the dielectric constant as a function of temperature behaves as that in ordinary nonferroelectric dielectrics: the dielectric constant decreases with temperature decreasing with the slope of $(1/\epsilon) d\epsilon/dT = +0.8 \cdot 10^{-4}$ and $+1.0 \cdot 10^{-4} \text{ K}^{-1}$ for SMN and SST, respectively. Similar value of $(1/\epsilon) d\epsilon/dT$ is characteristic for nonferroelectric oxides, alkali halides, and other ordinary dielectrics. This is in a great contrast with SrTiO_3 where $(1/\epsilon) d\epsilon/dT < 0$ and its absolute value is two and three orders of magnitude larger in ceramics and single crystals, respectively, as compared to $(1/\epsilon) d\epsilon/dT$ in SMN and SST. There is no frequency dispersion of the

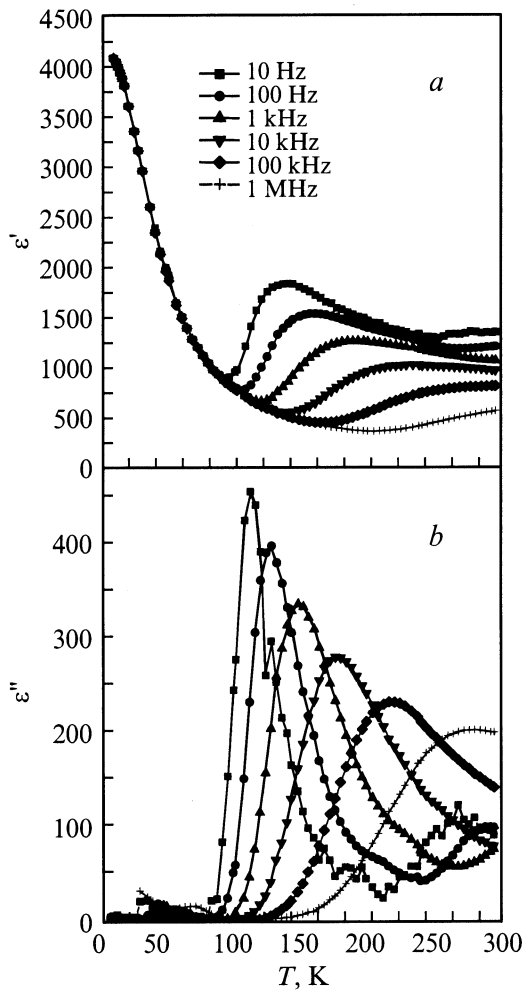


Figure 2. Temperature dependence of the real ϵ' (a) and the imaginary ϵ'' (b) parts of the dielectric constant in $(1-x)\text{SrTiO}_3-x\text{SrMg}_{1/3}\text{Nb}_{2/3}\text{O}_3$ at $x = 0.01$. Here and below, frequencies from top to bottom: 10 Hz, 100 Hz, 1 kHz, 10 kHz, 100 kHz, 1 MHz.

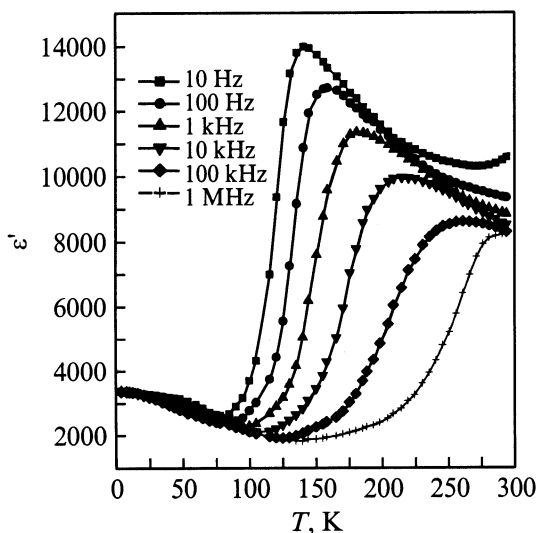


Figure 3. Temperature dependence of ϵ' in $(1-x)\text{SrTiO}_3-x\text{SrMg}_{1/3}\text{Nb}_{2/3}\text{O}_3$ at $x = 0.03$.

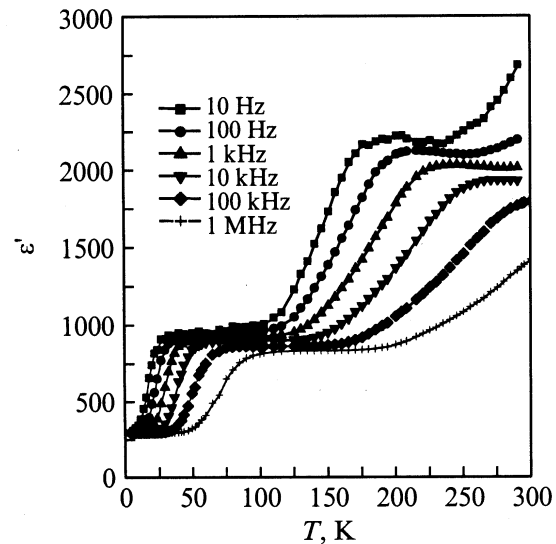


Figure 4. Temperature dependence of ϵ' in $(1-x)\text{SrTiO}_3-x\text{SrMg}_{1/3}\text{Nb}_{2/3}\text{O}_3$ at $x = 0.15$.

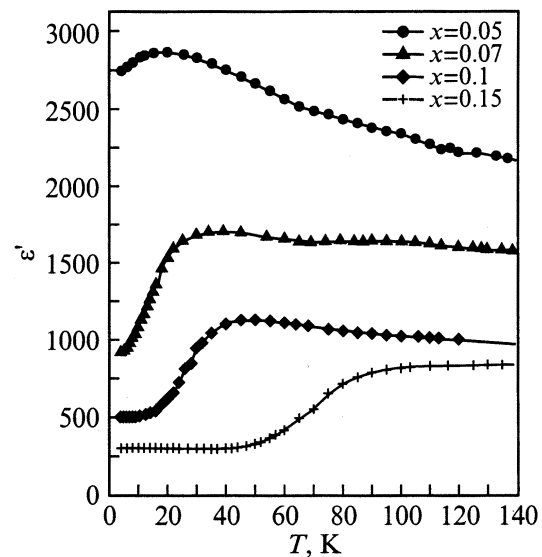


Figure 5. Temperature dependence of ϵ' in $(1-x)\text{SrTiO}_3-x\text{SrMg}_{1/3}\text{Nb}_{2/3}\text{O}_3$ at a frequency of 1 MHz. The x values from top to bottom: 0.05, 0.07, 0.1, 0.15.

dielectric constant both in SMN and SST, and in SrTiO_3 in the frequency range under study: 10 Hz–1 MHz. The situation drastically changes in the SrTiO_3 –SMN and SrTiO_3 –SST solid solutions. At the SMN concentration $x(\text{SMN}) = 0.005$, the first hints on a frequency dispersion (dielectric relaxation) appear both in ϵ' and ϵ'' frequency spectra and in ϵ' and ϵ'' temperature dependences. At $x = 0.01$, this relaxation becomes quite distinct (Fig. 2), and the relaxation features in this case are superimposed on the dielectric constant temperature dependence characteristic for the pure SrTiO_3 ceramics. It should be noted that

in the SrTiO_3 ceramic samples the maximum value of the dielectric constant at 4.2 K is usually several times less than in single crystals; in our samples this value is about 5000.

The relaxation strength attains the maximum at $x = 0.03$ (Fig. 3), and then decreases with x increasing. Along with this, — say, high-temperature, — relaxation which develops between 100 and 300 K, a low-temperature relaxation appears as x increases (Fig. 4), and the high value of the dielectric constant of SrTiO_3 becomes suppressed at $x \geq 0.03$. One can follow the evolution of this low-temperature relaxation in Fig. 5 where the $\epsilon'(T)$ dependences are shown at x between 0.05 and 0.15 at a frequency of 1 MHz.

Certainly, as well as in the ϵ' and ϵ'' temperature dependences, the dielectric relaxation reveals itself in ϵ' and ϵ'' frequency spectra. As an example, these spectra are shown for the high-temperature relaxation at $x = 0.03$

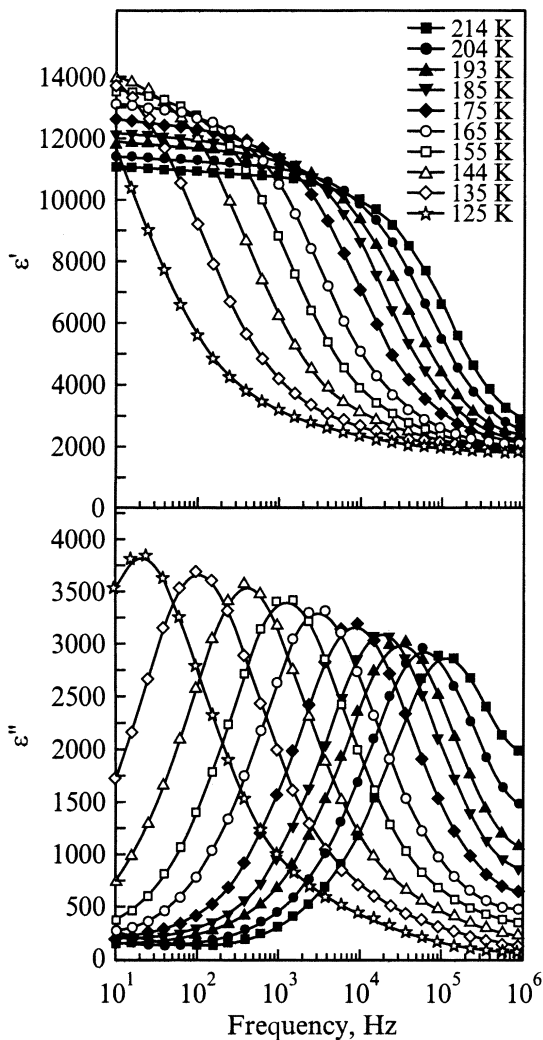


Figure 6. Frequency spectra of ϵ' and ϵ'' in $(1-x)\text{SrTiO}_3-x\text{SrMg}_{1/3}\text{Nb}_{2/3}\text{O}_3$ at $x = 0.03$. The high-temperature relaxation at various temperatures.

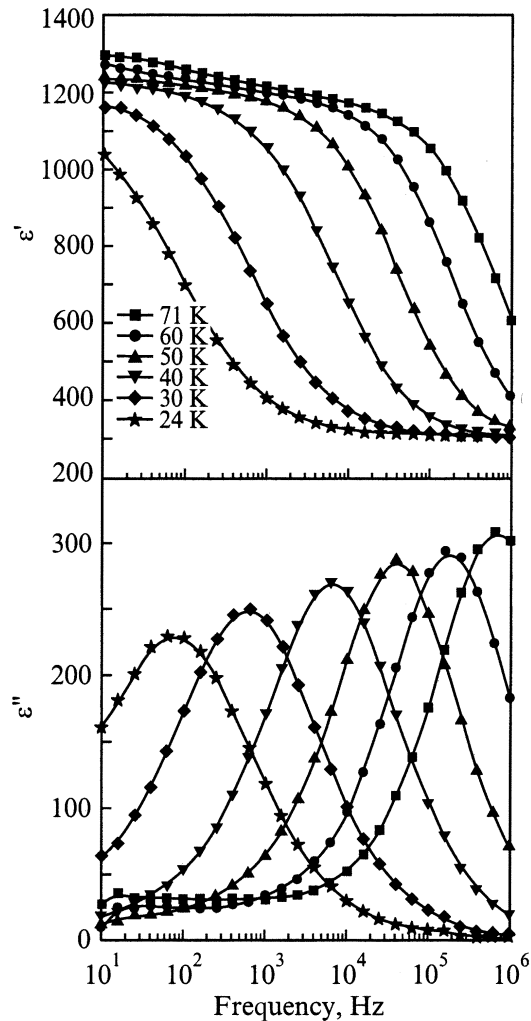


Figure 7. Frequency spectra of ϵ' and ϵ'' in $(1-x)\text{SrTiO}_3-x\text{SrMg}_{1/3}\text{Nb}_{2/3}\text{O}_3$ at $x = 0.15$. The low-temperature relaxation at various temperatures.

in Fig. 6 and for the low-temperature relaxation at $x = 0.15$ in Fig. 7.

The high-temperature dielectric relaxation was also observed in $(1-x)\text{SrTiO}_3-x\text{SST}$ solid solutions (Figs. 8, 9). The samples with $x = 0.01, 0.05,$ and 0.1 were measured. The most strong relaxation occurs at $x = 0.05$, and the relaxation disappears at $x = 0.1$.

In $\text{SrTiO}_3\text{-SMN}$ samples the relaxation is much stronger than that in $\text{SrTiO}_3\text{-SST}$.

The most remarkable feature of the high-temperature relaxation in Figs. 2–4, 6 is a very high value of the dielectric constant. At the SMN concentration $x(\text{SMN}) = 0.03$, the dielectric constant ϵ_0 attains the value of 14000 at 150 K, and around 1000 at 300 K. The relaxation strength ($\epsilon_0 - \epsilon_\infty$) is very high and varied roughly proportional to $1/T$ as can be seen in Figs. 2, 3.

All the temperature and frequency dependences in Figs. 2–9 look like classical, text book relaxation dependences. They demonstrate a typical Debye relaxation

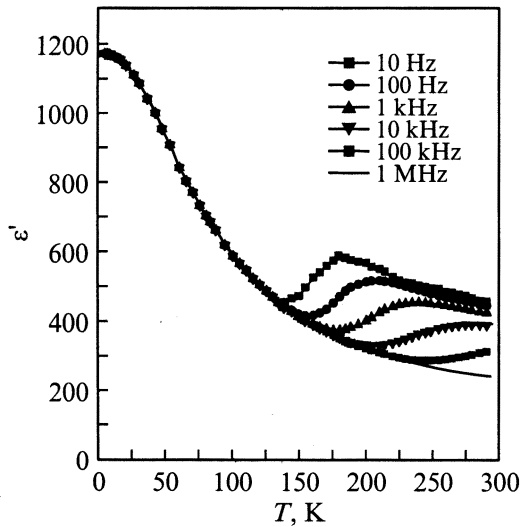


Figure 8. Temperature dependence of ε'' in $(1-x)\text{SrTiO}_3-x\text{SrSc}_{1/2}\text{Ta}_{1/2}\text{O}_3$ at $x = 0.01$.

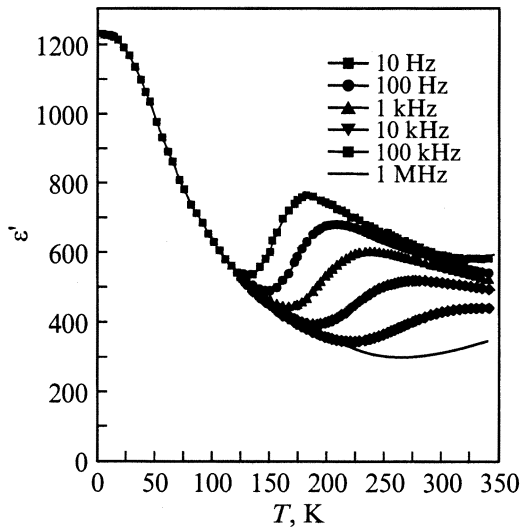


Figure 9. Temperature dependence of ε'' in $(1-x)\text{SrTiO}_3-x\text{SrSc}_{1/2}\text{Ta}_{1/2}\text{O}_3$ at $x = 0.05$.

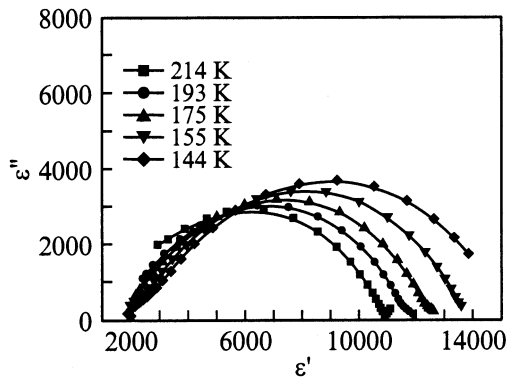


Figure 10. Cole-Cole plot in $(1-x)\text{SrTiO}_3-x\text{SrMg}_{1/3}\text{Nb}_{2/3}\text{O}_3$ at $x = 0.03$. The high-temperature relaxation at various temperatures.

Table 1. Activation energy U and relaxation time τ_0 in the high-temperature relaxation in $(1-x)\text{SrTiO}_3-x\text{SrMg}_{1/3}\text{Nb}_{2/3}\text{O}_3$ and $(1-x)\text{SrTiO}_3-x\text{SrSc}_{1/2}\text{Ta}_{1/2}\text{O}_3$

	x	U , eV	τ_0 , 10^{-11} s
SMN	0.01	0.23	5
	0.03	0.21	0.9
	0.05	0.23	0.3
	0.07	0.24	0.4
	0.1	0.26	0.2
	0.15	0.3	0.2
SST	0.01	0.27	1.5
	0.05	0.29	0.7

Table 2. Activation energy U and relaxation time τ_0 in the low-temperature relaxation in $(1-x)\text{SrTiO}_3-x\text{SrMg}_{1/3}\text{Nb}_{2/3}\text{O}_3$

x	U , eV	τ_0 , 10^{-9} s
0.07	0.02	0.3
0.1	0.01	0.2
0.15	0.02	15

behavior of the dielectric properties

$$\varepsilon' = \varepsilon_\infty + \frac{(\varepsilon_0 - \varepsilon_\infty)}{1 + \omega^2\tau^2},$$

$$\varepsilon'' = \frac{(\varepsilon_0 - \varepsilon_\infty)\omega\tau}{1 + \omega^2\tau^2}. \quad (1)$$

From the experimental data it follows that the relaxation time τ obeys an Arrhenius relation

$$\tau = \tau_0 \exp(U/kT). \quad (2)$$

Fitting the experimental data to Eqs. (1),(2), one obtains U and τ_0 which are presented in Tables 1 and 2.

In Table 1, one can see that in general there is a small but systematic increase in the activation energy U with x increasing. Interestingly, the similar behavior of $U(x)$ was observed in the case of SrTiO_3 doped with trivalent rare-earth ions [22].

A detail analysis shows that the experimental results can be described better by a Cole-Cole complex function instead of Eq. (1)

$$\varepsilon^* = \varepsilon_\infty + \frac{(\varepsilon_0 - \varepsilon_\infty)}{1 + (i\omega\tau)^\beta}, \quad (3)$$

where $\varepsilon^* = \varepsilon' - i\varepsilon''$.

As an example, one can see in Fig. 10 the Cole-Cole graph at $x(\text{SMN}) = 0.03$ and at various temperatures. The best fit of the experimental data to Eq. 3 is obtained with $\beta = 0.7$.

Fitting the experiment to Eq. (3) does not significantly change the values of U and τ_0 presented in Table 1.

Concerning the low-temperature relaxation, one should note that the experimental data can be fairly well fit by a simple Arrhenius relation (Eq. (2)) only at temperatures $T \geq 20$ K. The best fit in the whole temperature range may be obtained using a Vogel–Fulcher relation

$$\tau = \tau_0 \exp[U/k(T - T_g)] \quad (4)$$

with $U \approx 0.05$ eV but with $T_g < 0$. Since this value of T_g has no physical meaning we used the Arrhenius relation with the U and τ_0 values given in Table 2.

We also tried to observe $P(E)$ hysteresis loops in our samples at low temperatures. This attempt failed, and one may conclude that there are no ferroelectric phase transition in $\text{SrTiO}_3\text{-SMN}$ and $\text{SrTiO}_3\text{-SST}$ solid solutions.

3. Discussion

Thus, in the $(1-x)\text{SrTiO}_3\text{-}x\text{SMN}$ and $(1-x)\text{SrTiO}_3\text{-}x\text{SST}$ solid solutions we observed the strong high-temperature (150–300 K) dielectric relaxation; much smaller low-temperature (20–90 K) relaxation was also observed in the case of $\text{SrTiO}_3\text{-SMN}$. As mentioned before, the observed high-temperature relaxation in $\text{SrTiO}_3\text{-SMN}$ is characterized by very high dielectric constant ϵ_0 and very high relaxation strength $(\epsilon_0 - \epsilon_\infty)$ which at $x = 0.03$ and at a frequency of 10 Hz attain 14 000 and 12 000, respectively. Such a large value of ϵ_0 (larger than dielectric constant at 4.2 K in nominally pure SrTiO_3 ceramic samples) is surprising. These values are to our knowledge the highest yet reported for SrTiO_3 with heterovalent impurities in this temperature range. In the literature there has been only two examples [16,22] of very high value of ϵ_0 and $(\epsilon_0 - \epsilon_\infty)$ close to but less than the mentioned above. One of these examples is $\text{SrTiO}_3:2 \text{ at.}\% \text{Er}$ with $\epsilon_0 = 10\,000$ and $(\epsilon_0 - \epsilon_\infty) = 9400$ [22].

Very strong dielectric relaxation has been also observed in the other incipient ferroelectric, KTaO_3 . In KTaO_3 with 2.3 at.% Nb (KTN) and 0.055 at.% Ca dielectric relaxation was measured between about 50 and 100 K with ϵ_0 about 16 000 [28]. The similar value of ϵ_0 in the same temperature range was found in KTaO_3 with 2.5% Nb and 0.1% Li (KLTN) [29]. But in both cases [28,29] the dielectric relaxation develops close to a ferroelectric phase transition which, certainly, strongly affects the relaxation strength.

The dielectric constant of very large value is usually observed in SrTiO_3 at ferroelectric phase transitions induced by impurities at the impurity concentration x near the critical concentration x_c . For example, $\epsilon_m = 110\,000$ in $\text{SrTiO}_3:\text{Ca}$ single crystals at $x = 0.01$ [5] and $\epsilon_m = 170\,000$ in $\text{SrTiO}_3:^{18}\text{O}$ single crystals at $x = 0.37$ [30]. In ceramic samples of $\text{Sr}_{1-x}\text{Ba}_x\text{TiO}_3$ according to our measurements $\epsilon_m = 35\,000$ at $x = 0.02$. However, in the systems under study, $\text{SrTiO}_3\text{-SMN}$ and $\text{SrTiO}_3\text{-ST}$, there are no ferroelectric phase transitions, and the observed giant dielectric constant should be determined by some other mechanisms.

In discussing possible mechanisms of the giant dielectric relaxation, the first question to be answered is what positions occupy Nb^{5+} and Mg^{2+} in the SrTiO_3 host lattice. The Nb^{5+} ions should substitute for the Ti^{4+} host ions due to the size and charge factors. As for the Mg^{2+} ions, in principle, they can occupy either Sr^{2+} or Ti^{4+} positions. Two experimental facts prove the latter possibility. Firstly, the Mg^{2+} ions being added to SrTiO_3 alone (in the form of MgTiO_3) do not lead to any dielectric relaxation. Secondly, in the $\text{SrTiO}_3\text{-SMN}$ system, as well as in $\text{SrTiO}_3\text{-SST}$, the lattice constant follows the linear Vegard law between SrTiO_3 and SMN (SST). Thus, we make the conclusion that the Mg^{2+} and Nb^{5+} (or Sc^{3+} and Ta^{5+}) ions substitute for the host Ti^{4+} ions in SrTiO_3 . Though the impurity ions have charges different from that of the host Ti^{4+} ions, they are „self-compensating“, that is to say, the excess charge of two Nb^{5+} ions is compensated by the deficient charge of one Mg^{2+} ion and their average charge is equal to the charge of the host Ti^{4+} ion. The similar situation occurs in $\text{SrTiO}_3\text{-SST}$ where the excess charge of one Ta^{5+} ion is compensated by the deficient charge of one Sc^{3+} ion.

However, at small x , when the Mg^{2+} and Nb^{5+} ions (Sc^{3+} and Ta^{5+}) are far from each other, the Mg^{2+} ion „does not know“ that somewhere there are Nb^{5+} ions with compensating charge (with the same situation for the Nb^{5+} ions). Therefore, the impurity ions need some additional local charge compensation. This hypothesis is a basic point for explanation of dielectric relaxation in the systems under study. We believe that without this hypothesis of the additional local charge compensation it is impossible to suggest any models of the observed dielectric relaxation. The additional local charge compensation may proceed through formation of either free charge carriers or the host ion vacancies in the following ways.

Substituting for the host Ti^{4+} ion, Nb^{5+} (and Ta^{5+}) serves as a donor and Mg^{2+} (and Sc^{3+}) plays a role of an acceptor. Being fully ionized one Nb^{5+} and one Mg^{2+} provide one electron and two holes, respectively. If electron and hole mobility is equal, the electric conductivity will be compensated and the sample will have high resistivity. In the opposite case, the resistivity may be relatively low.

The second possible way of the local charge compensation is the formation of one Sr^{2+} vacancy (V_{Sr}) per each two Nb^{5+} ions and one O^{2-} vacancy (V_{O}) per each Mg^{2+} ion. In the case of SST, one Sr^{2+} vacancy should be formed per each two Ta^{5+} ions, and one O^{2-} vacancy is formed per each two Sc^{3+} ions.

These two means of the local charge compensation may lead to two mechanisms of the high-temperature (150–300 K) dielectric relaxation.

High electric conductivity may be a reason of the Maxwell–Wagner relaxation in ceramic samples, and it is well-known that strong dielectric relaxation in semiconducting ceramic samples may be always attributed to the Maxwell–Wagner mechanism. This relaxation is due to the different properties of ceramic grains and grain boundaries (see Ref. 31 and references therein). In a very simplified

model, the grain is considered as a resistor R with the grain boundary as an insulating layer with the capacity C in series with the resistor. A ceramic sample represents a system of such RC elements, and the relaxation time which is the effective Maxwell relaxation time of the whole system is given by

$$\tau = 8.8 \cdot 10^{-14} (\varepsilon_{\text{eff}}/\sigma). \quad (5)$$

where the relaxation time τ is in s and the electric conductivity σ is in $(\text{Ohm} \cdot \text{cm})^{-1}$.

The temperature dependence of conductivity $\sigma = en\mu$ is mainly determined by the temperature dependence of the charge carrier concentration

$$n = n_0 \exp(-U/kT). \quad (6)$$

The Maxwell–Wagner relaxation mechanism may give very high value of ε_{eff} at $\omega\tau < 1$.

The effective dielectric constant of a ceramic specimen is approximately given as [31]

$$\varepsilon_{\text{eff}} \cong (d_1/d_2)\varepsilon_2 \quad (7)$$

where d_1 is the grain size; d_2 the thickness of the grain boundary and ε_2 the dielectric constant of the grain boundary. With $d_1/d_2 \cong 10^2$ and $\varepsilon_2 \cong 10^2$, Eq. (7) gives $\varepsilon_{\text{eff}} \cong 10^4$.

The Maxwell–Wagner mechanism has been studied in detail for SrTiO₃ ceramics [31]. Ceramic samples of stoichiometric SrTiO₃ as well as with up to 1% excess of Ti were used. It was shown that the dielectric constant reached the value of about 10^4 at 150°C at a frequency of 10^{-2} Hz and that this value was due to the Maxwell–Wagner relaxation. Temperature-dependent maxima in $\varepsilon''(\omega)$ were observed which shifted to higher frequencies with increasing temperature. At 150°C, $\varepsilon''(\omega)$ attained the maximum value at a frequency about 1 Hz. Assuming reasonable (though rather arbitrary) values of parameters: $d_1 = 10$, $d_2 = 0.1 \mu\text{m}$, $\varepsilon_2 = 200$, carrier concentration $n_0 = 10^{18} \text{ cm}^{-3}$, mobility $\mu = 6 \text{ cm}^2/\text{V} \cdot \text{s}$, activation energy $U = 0.7 \text{ eV}$, the authors [31] obtained satisfactory agreement between the experimental results and the Maxwell–Wagner model.

The value of $U = 0.7 \text{ eV}$ is determined by the energy levels of donors or acceptors in the bandgap [31]. This energy is quite typical for SrTiO₃. To determine whether the relaxation in our samples which develops in 150–300 K range can be described by the Maxwell–Wagner model, one has to put this energy equal to $U \sim 0.25 \text{ eV}$. Then, using Eqs. (5)–(7) with d_1 , d_2 , and ε_2 from [31] and charge carrier mobility from [32], one obtains that the Maxwell–Wagner mechanism can satisfactorily describe the experimental results with the following values of conductivity and concentration. At 150 K, $\sigma \sim 10^{-5} (\text{Ohm} \cdot \text{cm})^{-1}$, $n \sim 10^{12} \text{ cm}^{-3}$, $n_0 \sim 5 \cdot 10^{20} \text{ cm}^{-3}$ and these quantities, σ and n , vary exponentially with temperature (Eq. (6)) with $U = 0.25 \text{ eV}$. Note that at $x = 0.03$, SMN concentration is $n \cong 5 \cdot 10^{20} \text{ cm}^{-3}$ which is not quite consistent with the value

of n_0 . Nevertheless, it is possible to conclude that the high-temperature dielectric relaxation may be associated with the Maxwell–Wagner mechanism.

However, there are the following experimental facts which contradict to the Maxwell–Wagner model of the dielectric relaxation in the 150–300 K temperature range.

According to Eq. (7), the dielectric constant is independent of temperature whereas the experiment demonstrates $1/T$ dependence.

At about 250 K and at a frequency of 10 Hz, one observes an increase of ε' with temperature increasing which may be the onset of an additional relaxation, especially distinct at $x = 0.15$ (Fig. 4). A crude estimate shows that for this relaxation $U \geq 0.5 \text{ eV}$. Just this relaxation may be ascribed to the Maxwell–Wagner model. Though nobody forbids to observe in one sample two Maxwell–Wagner relaxations in different temperature regions (say, at $T > 300 \text{ K}$ and at $T < 300 \text{ K}$), such an event seems to be rather accidental.

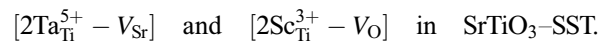
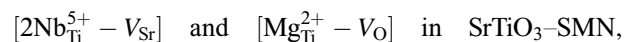
The observed dependence of the activation energy U on concentration x is difficult to explain in the framework of the Maxwell–Wagner mechanism as has been emphasized earlier [22].

Application of d.c. electric field $E = 1 \text{ kV/cm}$ does not change the relaxation under discussion but leads to great changes in ε'' and $\tan(\delta)$ at higher temperatures. At the SMN concentration $x = 0.05$, at $T = 275 \text{ K}$, and at a frequency of 1 kHz, ε'' increases by more than an order of magnitude under the action of the d.c. electric field.

The Maxwell–Wagner mechanism of the dielectric relaxation in SrTiO₃ with rare-earth ions [16,17,22] in the same temperature range as discussed above has been also denied. In SrTiO₃:La ceramics only relaxation at temperatures around 200°C has been associated with the Maxwell–Wagner mechanism [17]. Relaxation in 150–300 K range has been ascribed to formation of the host ion vacancies. One of the arguments against the Maxwell–Wagner mechanism for this relaxation was that the relaxation holds even in single crystals [17].

Now, we will discuss an alternative model of the giant dielectric relaxation based on the local charge compensation of impurities by the host ion vacancies as described above.

The electrostatic interaction makes the most favorable configuration when the impurity ions and related vacancies are the nearest neighbours. As a result one obtains such impurity centers



It is widely accepted that in the ABO₃ perovskites the mobility of the oxygen vacancies is higher than that of the A-ions [33], that is why we shall discuss below only the centers with the oxygen vacancies $[\text{Mg}_{\text{Ti}}^{2+} - V_{\text{O}}]$ and $[2\text{Sc}_{\text{Ti}}^{3+} - V_{\text{O}}]$. The $[\text{Mg}_{\text{Ti}}^{2+} - V_{\text{O}}]$ complex is shown in Fig. 11. The Mg²⁺ ion is in the center of the oxygen octahedron and one of six oxygen ions is absent (V_{O}). The Mg²⁺–O²⁻ distance is $a/2$ (a is the lattice parameter), the distance

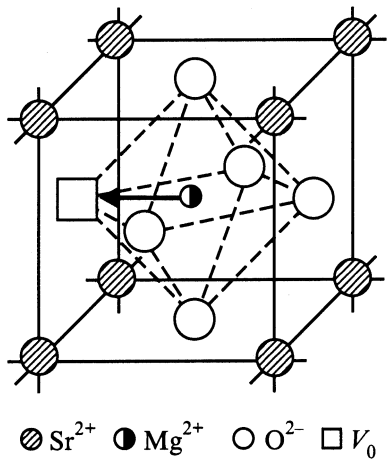


Figure 11. Structure of $[\text{Mg}_{\text{Ti}}^{2+}-\text{V}_0]$ center.

between the nearest O^{2-} ions is $a/\sqrt{2}$. The dipole moment $p = 2ea/2 = ea = 18.7 \cdot 10^{-18}$ (CGSE units) = $18.7D$ is associated with this center. Thermally activated reorientation of this dipole moment via the vacancy jumping (or, better to say, the oxygen ion jumping through the oxygen vacancy) is suggested as the origin of the dielectric relaxation with $U = 0.21\text{--}0.3$ eV and $\tau_0 = 10^{-11}\text{--}10^{-12}$ s. These relaxation parameters seem to be quite reasonable. Indeed in the model under discussion $\tau_0^{-1} = \omega_0$ should be of the order of magnitude of the lattice Debye frequencies. As for activation energy, $U \sim 0.25$ eV, at first sight it seems to be too low since the activation energy for the oxygen vacancy diffusion in the perovskite is not less than 1 eV [34,35]. However, it is well-known that the activation energy for the oxygen ion movement near a defect (as in our case) can be much lower. For example, in KTaO_3 , where the activation energy for d.c. ionic conductivity is also not less than 1 eV, the activation energy for oxygen vacancy hopping around defect is very low: $U = 0.08, 0.11,$ and 0.36 eV for the defect centers $[\text{Ca}_{\text{Ta}}^{2+}-\text{V}_0]$, $[\text{Mn}_{\text{Ta}}^{2+}-\text{V}_0]$, and $[\text{Co}_{\text{Ta}}^{2+}-\text{V}_0]$, respectively (Ref. 28 and references therein). Even for the reorientation of $\text{Fe}^{3+}-\text{O}_i^{2-}$ center in KTaO_3 with an interstitial oxygen ion O_i^{2-} , the activation energy is as low as 0.34 eV [36,37].

In the case of SrTiO_3 one may suppose similar situation and then the value of $U = 0.21\text{--}0.3$ eV seems to be quite reasonable. It is important to note that the activation energy around $U = 0.25$ eV has been found earlier in the dielectric relaxation in SrTiO_3 ceramics doped with Bi [11,12], Mn [20] with La [17,20–22], and other trivalent rare-earth ions [22]. The dielectric relaxation in all these systems was ascribed to the host ion vacancies.

In the model under discussion the relaxation strength $(\epsilon_0 - \epsilon_\infty)$ should decrease when the concentration x of SMN increases since the Mg^{2+} and Nb^{5+} ions will be close to each other, and their charge self-compensation will take place instead of the compensation by the vacancies. If the observed dielectric relaxation is due to this mechanism,

the relaxation strength, $(\epsilon_0 - \epsilon_\infty)$, should at first increase with x increasing, reach a maximum at a certain x and then decrease and completely disappear at large x . Just this behavior demonstrates the high-temperature relaxation in our samples.

The next important point is the unusually high relaxation strength $(\epsilon_0 - \epsilon_\infty)$. Let us estimate the relaxation strength in the framework of the proposed model. An electric field E induces a polarization P due to the reorientation of the $[\text{Mg}_{\text{Ti}}^{2+}-\text{V}_0]$ complex with the dipole moment $p = ea$ and the concentration n

$$P = (p^2 n / kT) E \quad (8)$$

with the dielectric susceptibility

$$\chi = p^2 n / kT. \quad (9)$$

Then, for $x = 0.03$ and assuming that all the Mg^{2+} impurity ions form the $[\text{Mg}_{\text{Ti}}^{2+}-\text{V}_0]$ centers, one obtains (in CGSE units) $\chi \cong 10$ or $\epsilon \cong 4\pi\chi \cong 10^2$. This value is too small to explain the experimental results. However, in Eq. (8) the local electric field E_{loc} should be taken instead of the applied electric field E .

As a crude estimation of the local field one can use the following expression [38]

$$E_{\text{loc}} = \left((\epsilon_\infty + 2) / 3 \right) E. \quad (10)$$

For the dielectric relaxation at $x = 0.03$, $\epsilon_\infty \approx 2000$ (Fig. 6), i.e. the local electric field is almost three orders of magnitude larger than the applied field. As a result one obtains $\epsilon \approx 2.5 \cdot 10^4$. Certainly, this value should be considered as an upper limit, and it only demonstrates that the proposed model can provide very high dielectric constant.

It is interesting to note that from the experiment [37] it appears that in $\text{KTaO}_3:\text{Fe}$, the local electric field at the $[\text{Fe}_{\text{K}}^{3+}-\text{O}_i]$ center is an order of magnitude larger than the applied field. This means that the local field in SrTiO_3 is much larger than in KTaO_3 .

As a result we may say that the proposed model is consistent with the experimental data: the model can, in principle, give the high value of ϵ_0 ; the experimental dependence of $\epsilon_0 \propto 1/T$ is explained by Eq. (9); the experimental activation energy U about 0.25 eV is in the range of typical values of the activation energy for oxygen vacancy jumping around impurity ion in perovskites.

Along with the high-temperature relaxation in the $\text{SrTiO}_3\text{-SMN}$, the low-temperature relaxation is observed with $U \sim 0.01\text{--}0.02$ eV and $\tau_0 \sim 10^{-8}\text{--}10^{-10}$ s. We believe that this activation energy is too low for the ion movement and should be attributed to the electronic system. The following model may be suggested to explain the low-temperature relaxation.

Some part of the Nb^{5+} ions is compensated not with the Sr^{2+} vacancies but forms a new center $[\text{Nb}_{\text{Ti}}^{5+}-\text{Ti}^{3+}]$ (Fig. 12). The Nb^{5+} ion is surrounded by six Ti^{4+} ions

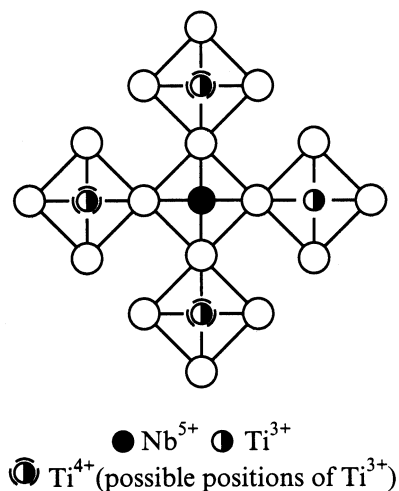


Figure 12. Structure of $[\text{Nb}_{\text{Ti}}^{5+}-\text{Ti}^{3+}]$ center.

and one of them is in the Ti^{3+} state, i.e., there is an electron localized on the Ti ion. This electron jumps over six Ti^{4+} ions. The distance between the Nb and Ti ions and between the Ti ions is a and $a\sqrt{2}$, respectively. The activation energy for this electron hopping can be sufficiently low. The excess electron polarizes the lattice and hops as a „polarization-dressed“ electron, i.e. as a polaron. In such a case, an accepted point of view [39] is that the relaxation time τ_0 should be between the characteristic lattice times ($\tau_0 = \omega_0^{-1} \cong 10^{-12}-10^{-13}$ s) and electronic times ($10^{-14}-10^{-15}$ s). However, we believe that for a polaron bounded to the impurity ion ($\text{Nb}_{\text{Ti}}^{5+}$ in our case) this relaxation time may be much larger — it can take much time for the lattice to come to the equilibrium after the electron hopping from one Ti ion to the other. Indeed, for example, in TiO_2 reduced crystals three relaxation processes associated with polaron hopping were observed [40] with the activation energy between 10^{-3} and 10^{-2} eV and τ_0 between 10^{-8} and 10^{-6} s. Thus, our values of U and τ_0 seem to be reasonable.

Now, let us turn to the SrTiO_3 -SST solid solution. The high-temperature relaxation is also observed in this system but the relaxation strength is much smaller than that for the SrTiO_3 -SMN. The $[2\text{Sc}_{\text{Ti}}^{3+}-V_{\text{O}}]$ center has rather a complicated structure to provide easy movement of the oxygen vacancy. But some small part of these centers can exist as a simple $[\text{Sc}_{\text{Ti}}^{3+}-V_{\text{O}}]$ center. If so, the relaxation mechanism will be the same as for the $[\text{Mg}_{\text{Ti}}^{2+}-V_{\text{O}}]$ centers but with much smaller relaxation strength due to small concentration of the $[\text{Sc}_{\text{Ti}}^{3+}-V_{\text{O}}]$ centers.

Discussing the dielectric relaxation associated with the thermally activated movement of the host ion vacancies, one should, certainly, remind Skanavi's relaxation mode [11,12]. This model postulates that the Sr^{2+} ion vacancies distort the neighbouring oxygen octahedra and as a result several off-center equilibrium positions for the Ti^{4+} ion appear. The dielectric relaxation in this model is associated with

thermally activated motion of the Ti^{4+} ion between these equivalent off-center positions. In SrTiO_3 doped with La [17], La and Mn [20], and with a wide range of the rare-earth ions [22], the observed dielectric relaxation was explained in terms of Skanavi's model. However, this purely qualitative model is difficult to accept since it is doubtful that an asymmetric distortion of the oxygen octahedron may lead to several equivalent off-center positions for the Ti^{4+} ion. One needs theoretical microscopic calculations to support this model. That is why we did not discuss this model as a possible reason of the dielectric relaxation. And what is more, the authors of the recent paper [16] argue that the experimental results on the dielectric relaxation in SrTiO_3 are not consistent with Skanavi's model.

In conclusion, in SrTiO_3 - $\text{SrMg}_{1/3}\text{Nb}_{2/3}\text{O}_3$ and in SrTiO_3 - $\text{SrSc}_{1/2}\text{Ta}_{1/2}\text{O}_3$ solid solutions the giant high-temperature (100–350 K) dielectric relaxation and not so strong but well developed low-temperature (20–90 K) relaxation were observed instead of a ferroelectric phase transition induced by impurities in the incipient ferroelectric and quantum paraelectric SrTiO_3 . This means that not any impurity can disturb the stability of the paraelectric phase in SrTiO_3 and induce a ferroelectric phase transition (otherwise one could tell about „impurity trigger effect“). In all the incipient ferroelectric-based solid solutions studied earlier [3–9], the second-end members of the solid solutions were ferroelectrics (BaTiO_3 , PbTiO_3 , CdTiO_3 , $\text{PbMg}_{1/3}\text{Nb}_{2/3}\text{O}_3$ in SrTiO_3 , and LiTaO_3 , KNbO_3 in KTaO_3) or at least incipient ferroelectrics as KTaO_3 and CaTiO_3 in SrTiO_3 [5,41,42]. In all these cases a transition to ferroelectric (or polar) phase inevitably occurred. In the present case, SMN and SST are not ferroelectrics which may be the reason of the absence of a ferroelectric phase transition in their solid solutions with SrTiO_3 . This point of view may be supported by [22], where SrTiO_3 with all the rare-earth ions except promethium was studied and no evidence of the ferroelectric state was found. It may imply that in the incipient ferroelectrics with impurities, the ferroelectric phase transition is due not to the impurity-trigger effect but is simply a Vegard-type law for the $T_c(x)$ dependence at medium and large values of the concentration x of the second-end member of the incipient ferroelectric-based solid solution. At low x , the transition to the quantum ferroelectric state occurs with no ferroelectric phase transition at x lower than the critical concentration x_c .

Returning to the dielectric relaxation in the solid solutions under study, one may conclude that both the Maxwell–Wagner mechanism and the reorienting dipole-center model may explain the main features of the high-temperature relaxation. There are some arguments in the favour of the model of the reorienting dipole centers but this conclusion is anything but final since using only dielectric measurements one cannot determine the structure of defect centers.

Finally, and most importantly, the both models are founded on the hypothesis of the additional local charge compensation of the heterovalent B-ions by the host ion vacancies or by free charge carriers. This scenario seems to be inevitable to explain the dielectric relaxation in the

solid solutions under study. However, in this context, more experimental proofs are desirable. These proofs may be provided by experiments with $\text{SrTiO}_3\text{-SMN}$ single crystals or/and using $\text{SrMn}_{1/2}\text{Nb}_{2/3}\text{O}_3$ instead of $\text{SrMg}_{1/3}\text{Nb}_{2/3}\text{O}_3$ to get the possibility of ESR study of Mn^{2+} centers. These, and not so simple, experiments are now in progress.

In the connection with this model of the additional local charge compensation, it is worth noting that a question is not ruled out whether this compensation may play any role in dielectric properties of disordered relaxor ferroelectrics such as $\text{PbMg}_{1/3}\text{Nb}_{2/3}\text{O}_3$ (PMN).

One of the authors (V.V.L.) would like to thank O.E. Kvyatkovskii and V.K. Yarmarkin for useful discussions.

At Ioffe Institute this work was partly supported by the Program „Physics of Solid State Nanostructures“ and NWO grant N 16-04-1999. One of the authors (E.P.S.) is grateful to Sächsisches Staatsministerium für Wissenschaft und Kunst for financial support.

References

- [1] K.A. Müller, H. Burkhard. *Phys. Rev.* **B19**, 3593 (1979).
- [2] H. Uwe, T. Sakudo. *Phys. Rev.* **B13**, 271 (1976).
- [3] V.V. Lemanov, *Fiz. Tverdogo Tela (St.Petersburg)* **39**, 1645 (1997). [*Phys. Solid State* **39**, 1468 (1997)].
- [4] V.V. Lemanov. *Ferroelectrics* **226**, 133 (1999).
- [5] J.G. Bednorz, K.A. Müller. *Phys. Rev. Lett.* **52**, 2289 (1984).
- [6] V.V. Lemanov, E.P. Smirnova, E.A. Tarakanov, P.P. Syrnikov, *Phys. Rev.* **B54**, 3151 (1996).
- [7] V.V. Lemanov, E.P. Smirnova, E.A. Tarakanov. *Fiz. Tverdogo Tela (St.Petersburg)* **39**, 714 (1997). [*Phys. Solid State* **39**, 628 (1999)].
- [8] M.E. Guzhva, V.V. Lemanov, P.A. Markovin, T.A. Shaplygina. *Ferroelectrics* **218**, 93 (1998).
- [9] V.V. Lemanov, A.V. Sotnikov, E.P. Smirnova, M. Weihnacht, W. Hässler. *Fiz. Tverdogo Tela (St.Petersburg)* **41**, 1091 (1999). [*Phys. Solid State* **41**, 994 (1999)].
- [10] Chen Ang, Zhi Yu, P.M. Vilarinho, J.L. Baptista. *Phys. Rev.* **57**, 7403 (1998).
- [11] G.I. Skanavi, E.N. Matveeva. *ZhETF* **30**, 6, 1047 (1956). [*Sov. Phys. JETP* **3**, 905 (1957)].
- [12] G.I. Skanavi, I.M. Ksendzov, V.A. Trigubenko, V.G. Prokhvatilov. *ZhETF* **33**, 2, 321 (1957). [*Sov. Phys. JETP* **6**, 250 (1958)].
- [13] Chen Ang, J.F. Scott, Zhi Yu., H. Ledbetter, J.L. Baptista. *Phys. Rev.* **B59**, 6661 (1999).
- [14] Chen Ang, Zhi Yu, J. Hemberger, P. Lunkenheimer, A. Loidl. *Phys. Rev.* **B59**, 6665 (1999).
- [15] Chen Ang, Zhi Yu, P. Lunkenheimer, J. Hemberger, A. Loidl. *Phys. Rev.* **B59**, 6670 (1999).
- [16] Chen Ang, Zhi Yu, L.E. Cross. *Phys. Rev.* **B62**, 228 (2000).
- [17] T.Y. Tien, L.E. Cross. *Jpn. J. Appl. Phys.* **6**, 459 (1967).
- [18] J. Bouwma, K.J. De Vries, A.J. Burggraaf. *Phys. Stat. Sol.* **A35**, 281 (1976).
- [19] Ang Chen, Yu Zhi. *J. Appl. Phys.* **71**, 6025 (1992).
- [20] E. Iguchi, K.J. Lee. *J. Mater. Sci.* **28**, 5809 (1993).
- [21] Zhi Yu, Chen Ang, L.E. Cross. *Appl. Phys. Lett.* **74**, 3044 (1999)
- [22] D.W. Johnson, L.E. Cross, A. Hummel. *J. Appl. Phys.* **41**, 2828 (1970).
- [23] Chen Ang, J.R. Jurado, Zhi Yu, M.T. Colomer, J.R. Frado, J.L. Baptista. *Phys. Rev.* **B57**, 11 858 (1998).
- [24] Chen Ang, Zhi Yu, Zhi Jing, P. Lukenheimer, A. Loidl. *Phys. Rev.* **B61**, 3922 (2000).
- [25] V.V. Lemanov, E.P. Smirnova, A.V. Sotnikov, M. Weihnacht. *Appl. Phys. Lett.* **77**, 4205 (2000).
- [26] F.S. Galasso. *Structure, Properties and Preparation of Perovskite-type Compounds*. Pergamon Press, Oxford (1969).
- [27] Powder Diffraction File, *Inorganic Phases*, 1989 (International Center for Diffraction Data, 1601 Park Lane, Swarthmore, PA 19081-238).
- [28] G.A. Samara, L.A. Boatner. *Phys. Rev.* **B61**, 3889 (2000).
- [29] V.A. Trepakov, M.E. Savinov, S. Kapphan, V.S. Vikhnin, L. Jastrabik, L.A. Boatner. *Ferroelectrics* **239**, 305 (2000).
- [30] M. Itoh, R. Wang. *Appl. Phys. Lett.* **76**, 221 (2000).
- [31] H. Neumann, G. Arlt. *Ferroelectrics* **69**, 179 (1986).
- [32] H.P.R. Frederikse, W.R. Hosler. *Phys. Rev.* **161**, 822 (1967).
- [33] A. Seuter. *Philips. Res. Repts. Suppl.* **3**, 1 (1974).
- [34] G. Arlt, H. Neumann. *Ferroelectrics* **87**, 109 (1988).
- [35] I. Sakaguchi, H. Honeda, S. Hishita, F. Watanabe, J. Tanaka. *Nucl. Instr. and Meth.* **B94**, 411 (1994).
- [36] V.S. Vikhnin, A.S. Polkovnikov, H.J. Reyher, B. Faust, S. Kapphan. *J. Korean Phys. Soc.* **32**, S486 (1998).
- [37] L.S. Sochava, V.E. Bursian, A.G. Razdobarin. *Fiz. Tverd. Tela (St.Petersburg)* **42**, 1595 (2000). [*Phys. Solid State* **42**, 1640 (2000)].
- [38] Ch. Kittel. *Introduction to Solid State Physics*. John Wiley & Sons, Inc., N.Y.–London–Sydney–Toronto.
- [39] M. Fisher, A. Lahmar, M. Maglione, A. San Miguel, J.P. Itie, A. Polian, F. Baudelet. *Phys. Rev.* **B49**, 12 451 (1994).
- [40] L.A.K. Dominik, R.K. MacCrone. *Phys. Rev.* **163**, 756 (1967).
- [41] V.V. Lemanov, V.A. Trepakov, P.P. Syrnikov, M. Savinov, L. Jastrabik. *Fiz. Tverd. Tela (St.Petersburg)* **39**, 1838 (1997). [*Phys. Solid State* **39**, 1642 (1997)].
- [42] V.V. Lemanov, A.V. Sotnikov, E.P. Smirnova, M. Weihnacht, R. Kunze. *Solid State Commun.* **110**, 611 (1999).